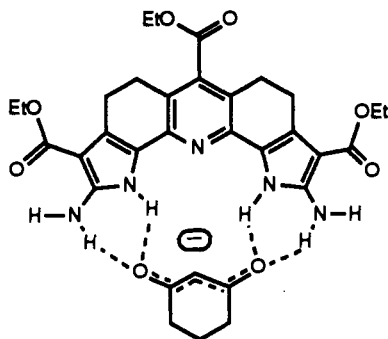


obvious ^1H or ^{13}C NMR resonances could distinguish **5a** from **5b**. Thus, a ^{13}C - ^{13}C correlated NMR spectrum²¹ was run on **5**, and tracing carbons a, b, and c yields the regiochemistry as shown for **5b**.^{20b}

When 15-crown-5 sodium enolates of 1,3-diketone functionalities are incrementally titrated into a solution of 1.0×10^{-3} M **1** and 2.0×10^{-3} M **5b** in acetonitrile- d_3 , the NH and NH_2 ^1H NMR resonances shift to lower field, typically over a range of 1.5 and 0.7 ppm, respectively. The binding constants calculated with the typical binding algorithm²² are shown in Table I. Compound **1** binds each anion significantly better than **5b**, reflecting the cooperativity between the two symmetric halves of **1**. The successful complexation reflects several interactions. The first is a lack of strong hydrogen bonding between the solvent and the enolates. The second is completely cooperative hydrogen bonding between relatively acidic NH and NH_2 groups and the basic enolate oxygens. As Whitlock discussed,²³ the more basic the hydrogen-bond acceptor, the stronger the complexation. However, we found that the correlation between basicity and binding strength does not hold when the hydrogen-bond acceptors are of different structure. Of the anions studied, malononitrile anion is the most basic,²⁴ but has the lowest binding constant. This is probably due to fewer hydrogen bonding contacts with **1**, or possibly increased association with the 15-crown-5 sodium. However, the fact that the enolate is relatively "naked"²⁵ and has little ability to coordinate to the counter sodium ion in a 15-crown-5 undoubtedly enhances complexation with **1**. Studies to confirm these effects are underway.

The proposed complexation geometry of 1,3-cyclohexanedionate with **1** is shown below.²⁶



Of the enolates tested, this one binds the strongest to **1**. This is likely due to the rigid structure of the enolate, which diverges the keto oxygens in an optimum manner to complement the convergence of the host hydrogen-bond donors of **1**. In contrast, the enolates of 2,4-pentanedione and 2-acetylcyclohexanone were found not to bind, due to increased conformational freedom over the other guests, and the preferred anti conformation of oxygens.²⁷

Enolization catalysts²⁸ and enolate-binding synthetic hosts such as **1** have the potential for controlling the regiochemistry, stere-

ochemistry, and kinetic reactivity of reactions involving enolates. Studies using **1** as a catalyst and the enolates discussed as transition-state analogues are in progress.

Acknowledgment. We gratefully acknowledge financial support for this project from the Texas Advanced Technology Program and an NSF-PYI award to E.V.A.

Gradient-Enhanced HMQC and HSQC Spectroscopy. Applications to ^{15}N -Labeled Mnt Repressor

Geerten W. Vuister,^{†,‡} Rolf Boelens,[†] Robert Kaptein,[†] Ralph E. Hurd,[§] Boban John,[§] and Peter C. M. Van Zijl*

Department of Chemistry, Bijvoet Center for Biomolecular Research, University of Utrecht Padualaan 8, 3584 CH Utrecht, The Netherlands
General Electric NMR
P.O. Box 4905, Fremont, California 94539
Department of Pharmacology
Georgetown University Medical School
4 Research Court, Rockville, Maryland 20850
Received July 5, 1991

The availability of high-quality shielded gradients for high-resolution NMR has provided new approaches to attain coherence selection¹ and water suppression.² Gradient techniques hold promise particularly for heteronuclear ^1H detected experiments (e.g., HMQC³ and HSQC⁴), where coherence of protons not bound to the heteronucleus is usually canceled by subtraction in consecutive scans. Gradient techniques can select for the desired coherence-transfer pathway in a single scan, while dephasing signals arising from other pathways. Thus, an inherent frequency-independent solvent suppression is attained when sufficient gradient strength is available. Compared to presaturation, there is the advantage that the time for magnetization transfer from saturated water to exchangeable protons is very short, allowing efficient detection of, for instance, amides in proteins.

We present the gradient-enhanced HMQC^{1g-i} and a novel gradient-enhanced HSQC experiment and apply them to ^{15}N -labeled Mnt repressor (1-76) (dimer, $M_w = 17\,500$) in $^1\text{H}_2\text{O}$ solution. Spectra are obtained with inherent $^1\text{H}_2\text{O}$ suppression in only 150 s, illustrating for the first time that these techniques are feasible for studying exchangeable protons in biomolecules.

The ratio of gyromagnetic ratios ($\gamma_{^1\text{H}}/\gamma_{^{15}\text{N}} = 9.88$) determines the phase acquired during t_1 and t_2 and thus the relative gradient strengths necessary to attain proper rephasing of the required coherence. In the gradient-enhanced HMQC experiment (Figure

* Georgetown University Medical School. Address correspondence to this author.

[†] University of Utrecht.

[‡] Present address: Laboratory of Chemical Physics, NIDDK, National Institutes of Health, Bethesda, MD 20892.

[§] General Electric NMR.

(1) (a) Bax, A.; De Jong, P. G.; Mehlkopf, A. F.; Smidt, J. *J. Chem. Phys. Lett.* **1980**, *69*, 567. (b) Counsell, C. J. R.; Levitt, M. H.; Ernst, R. R. *J. Magn. Reson.* **1985**, *64*, 470. (c) Sotak, C. H.; Freeman, D.; Hurd, R. E. *J. Magn. Reson.* **1988**, *78*, 355. (d) Knüttel, A.; Kimmich, R.; Spohn, K.-H. *J. Magn. Reson.* **1990**, *86*, 526. (e) Hurd, R. E. *J. Magn. Reson.* **1990**, *87*, 422. (f) Von Kienlin, M.; Moonen, C. T. W.; Van der Toorn, A.; Van Zijl, P. C. M. *J. Magn. Reson.* **1991**, *93*, 423. (g) Hurd, R. E.; John, B. *J. Magn. Reson.* **1991**, *91*, 648. (h) Swanson, S.; Yeung, H. N., 31st Experimental NMR Conference, 1990, p 197. (i) Knüttel, A.; Spohn, K.-H.; Kimmich, R. *Magn. Reson. Med.* **1991**, *17*, 470. (j) Brereton, I. M.; Crozier, S.; Field, J.; Doddrell, D. M. *J. Magn. Reson.* **1991**, *93*, 54.

(2) (a) Van Zijl, P. C. M.; Moonen, C. T. W. *J. Magn. Reson.* **1990**, *87*, 18. (b) Moonen, C. T. W.; Van Zijl, P. C. M. *J. Magn. Reson.* **1990**, *88*, 28. (c) Van Zijl, P. C. M.; Moonen, C. T. W. *NMR, Basic Principles & Progress*; Seelig, J., Rudin, M., Eds.; Springer Verlag: Berlin, Heidelberg, Vol. 26, in press. (d) Kaiser, R.; Bartholdi, E.; Ernst, R. R. *J. Chem. Phys.* **1974**, *60*, 2966. (e) Haase, A.; Frahm, J.; Hänicke, W.; Matthaei, D. *Phys. Med. Biol.* **1985**, *30*, 341. (f) Doddrell, D. M.; Galloway, D. J.; Brooks, W. M.; Field, J.; Bulsing, J. M.; Irving, M. G.; Baddeley, H. *J. Magn. Reson.* **1986**, *70*, 176. (3) (a) Müller, L. *J. Am. Chem. Soc.* **1979**, *101*, 4481. (b) Bax, A.; Griffey, R. H.; Hawkins, B. L. *J. Am. Chem. Soc.* **1983**, *105*, 7188. (c) Bax, A.; Griffey, R. H.; Hawkins, B. L. *J. Magn. Reson.* **1983**, *55*, 301. (4) Bodenhausen, G.; Ruben, D. *J. Chem. Phys. Lett.* **1980**, *69*, 185.

(21) Bax, A.; Freeman, R.; Kempell, S. P. *J. Am. Chem. Soc.* **1980**, *102*, 4849.

(22) (a) Wilcox, C. S.; Cowart, M. D. *Tetrahedron Lett.* **1986**, *27*, 5563-5566. (b) H. W. Whitlock, Jr., kindly provided the program. Sheridan, R. E.; Whitlock, H. W., Jr. *J. Am. Chem. Soc.* **1986**, *108*, 7120-7121, ref 8. Reference 8.

(23) Neder, K. M.; Whitlock, H. W., Jr. *J. Am. Chem. Soc.* **1990**, *112*, 9412-9414.

(24) Gordon, A. J.; Ford, R. A. *The Chemist's Companion*; John Wiley and Sons: New York, 1972.

(25) (a) Floriani, C.; Veya, P. *Organometallics* **1991**, *10*, 1652-1654. (b) Willard, P.; Carpenter, G. B. *J. Am. Chem. Soc.* **1986**, *108*, 462. (c) Pierre, J.-L.; Le Goeller, R.; Handel, H. *J. Am. Chem. Soc.* **1978**, *100*, 8021. (d) Riche, C.; Pascard-Billy, C.; Cambillau, C.; Bram, G. *J. Chem. Soc., Chem. Commun.* **1977**, 183.

(26) Floppy hosts often do not allow good host-guest structural predictions. See ref 14b and the following Cram, D. J. *Angew. Chem., Int. Ed. Engl.* **1986**, *25*, 1039.

(27) Bernasconi, C. F.; Kanavarioti, A. *J. Am. Chem. Soc.* **1986**, *108*, 7744-7751.

(28) (a) Tadayoni, B. M.; Huff, J.; Rebek, J., Jr. *J. Am. Chem. Soc.* **1991**, *113*, 2247-2253. (b) Wolfe, J.; Muehldorf, A.; Rebek, J., Jr. *J. Am. Chem. Soc.* **1991**, *113*, 1453-1454.

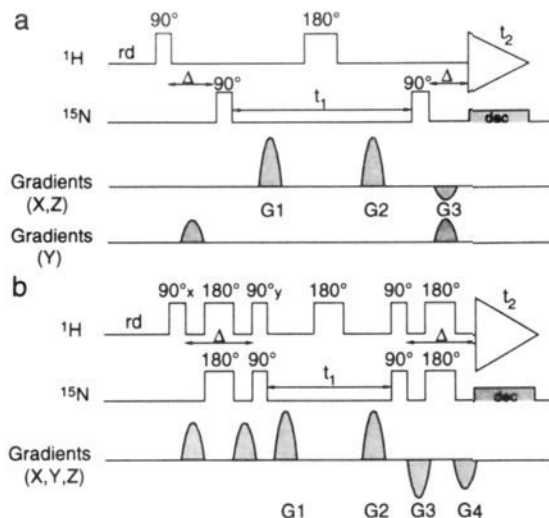


Figure 1. (a) Gradient-enhanced HMQC experiment. Relative strength for x,z gradients was G1:G2:G3 = 4.94:4.94:1; y gradients had relative amplitude 1.5; rd = 1 s; $\Delta = 1/[2J(^{15}\text{N}-^1\text{H})]$; dec denotes low-power Garp decoupling (1.7 kHz). (b) Gradient-enhanced HSQC experiment. Relative strength of x,y,z gradients was G1:G2:G3:G4 = 1:3.94:2.5:2.0. Two additional gradients with relative amplitude 2 surround the first $^{15}\text{N}/^1\text{H}$ 180° pulses.

1a), the effective result of evolution during t_1 is pseudo single-quantum (SQ) ^{15}N coherence.^{3c} During t_2 SQ proton coherence evolves. Thus, G1:G2:G3 = 4.94:4.94:±1 are possible combinations for proper rephasing. In HSQC experiments⁴ (Figure 1b), SQ coherence evolves during both t_1 and t_2 . Thus, G1:G2:G3:G4 = 0:9.88:-1:0 presents a possible combination. However, to avoid $^1\text{H}_2\text{O}$ signals resulting from imperfect 180° pulses, additional gradients (G1 and G4) were used. For both experiments, unwanted gradient-recalled echoes (e.g., from the coherently dephased $^1\text{H}_2\text{O}$ resonance) were avoided by empirically optimizing combinations of different gradient directions. A detailed account of the many possible gradient combinations and their experimental implications, e.g., for the occurrence/removal of artifacts, will be given elsewhere.

Figure 2 shows gradient-enhanced HMQC and HSQC spectra of Mnt repressor. The $^1\text{H}_2\text{O}$ resonance is suppressed to the level of the protein signals, avoiding dynamic range, radiation damping,^{2c} and base-line problems. The signal acquired is sufficient to detect 75% of the $^{15}\text{N}-^1\text{H}$ correlations of Mnt, comparable to a four-scan HMQC at 500 MHz.⁵ The loss of other cross peaks is attributed to reduced signal-to-noise due to the short experiment time and the low field strength used. The projections along ω_1 and ω_2 show that neither tails of residual $^1\text{H}_2\text{O}$ nor base-line roll is present. Signal-to-noise is slightly less for the HSQC compared to that for the HMQC, and some artifacts are visible (e.g., between 95 and 115 ppm). Both effects are due to \mathbf{B}_1 inhomogeneity in our experimental probe setup. Most signal loss is due to imperfections in the 180° pulses in the second delay Δ , where the gradient pair removes improperly refocused signals. Since absolute-value detection is used, these pulses can in principle be deleted. The artifacts are due to inaccuracies in the 180° proton pulse during t_1 and present different coherence pathways. They can be removed by replacing this pulse with ^1H decoupling during t_1 .

The results show that fast gradient-enhanced HSQC and HMQC experiments with inherent $^1\text{H}_2\text{O}$ suppression can be performed straightforwardly with high-quality shielded gradients. This will be important for the study of amide-exchange kinetics by 2D heteronuclear spectroscopy. One present disadvantage is that only phase-modulated signals in t_1 are obtained and spectra have to be displayed in absolute-value mode, resulting in a factor of $2^{1/2}$ signal loss with respect to conventional methods. However,

(5) Burgering, M. (unpublished results), private communication.

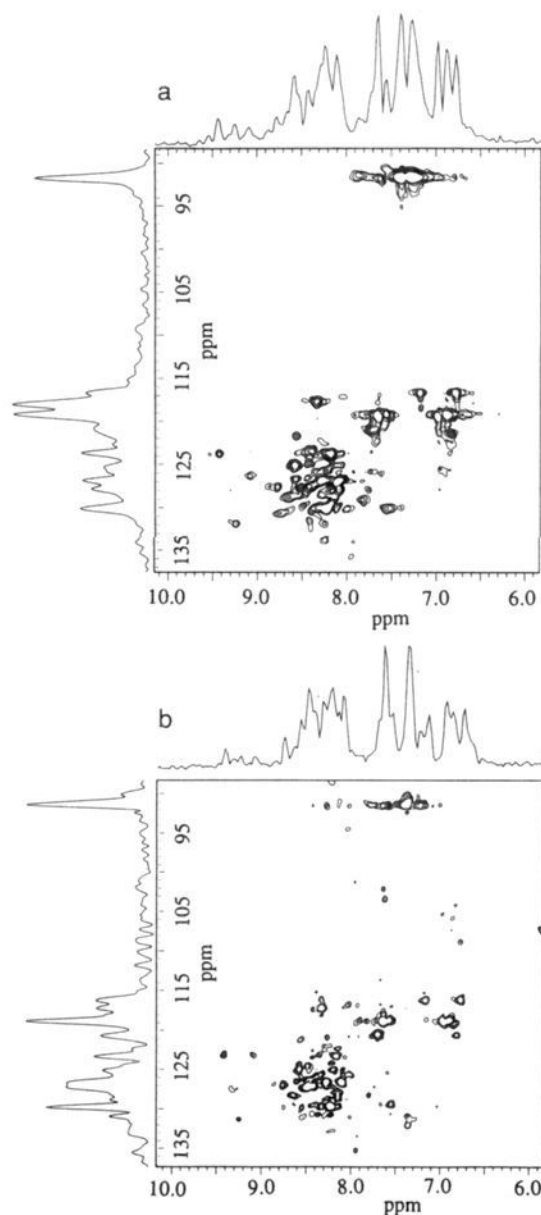


Figure 2. Absolute-value (a) HMQC and (b) HSQC spectra of 2 mM ^{15}N -labeled Mnt repressor in 95:5 v/v $^1\text{H}_2\text{O}/\text{D}_2\text{O}$ (room temperature, pH = 4.5). Experiments were recorded on a GE PSG high-resolution wide-bore 400-MHz NMR instrument equipped with shielded gradients. Relative gradient strength "1" (cf. Figure 1) of a sine-shaped gradient pulse corresponds to 0.129, 0.131, and 0.108 Tm^{-1} for x , y , and z , respectively. Gradient lengths of 2 ms and postgradient delays of 50 μs lead to a minimal t_1 value of 4.1 ms; 128 single-scan FIDs of 512 complex points, preceded by four dummy scans, were obtained in 150 s. Sine-bell windows shifted by 45° were used in t_1 and t_2 . Zero filling in t_1 yielded spectra of 256×512 complex points. No base-line-correction routines were applied. Projections along ω_1 and ω_2 are shown on the top and left-hand side, respectively.

application of a series of gradients during acquisition⁶ may present a way to overcome this limitation. Clearly, the aforementioned advantages of gradient techniques will be beneficial for heteronuclear 3D⁷ and 4D⁸ NMR. When more scans are necessary to

(6) Hurd, R. E.; John, B. K.; Plant, H. D. *J. Magn. Reson.* **1991**, *93*, 666.
 (7) (a) Fesik, S. W.; Zuiderweg, E. R. P. *J. Magn. Reson.* **1988**, *78*, 588.
 (b) Marion, D.; Kay, L. E.; Sparks, S. W.; Torchia, D. A.; Bax, A. *J. Am. Chem. Soc.* **1989**, *111*, 1515.
 (8) (a) Kay, L. E.; Clore, G. M.; Bax, A.; Gronenborn, A. M. *Science* **1990**, *249*, 411. (c) Clore, G. M.; Kay, L. E.; Bax, A.; Gronenborn, A. M. *Biochemistry* **1991**, *30*, 12. (c) Zuiderweg, E. R. P.; Petros, A. M.; Fesik, S. W.; Olejniczak, E. T. *J. Am. Chem. Soc.* **1991**, *113*, 370.

improve signal-to-noise, single-scan methods are also useful to increase digital resolution.

Acknowledgment. This research was supported by Pharmagenics, Inc., and the Netherlands Foundation for Chemical Research (SON) with the aid of the Netherlands Organisation of Scientific Research (NWO). The shielded gradients that made this study possible were provided by GE NMR Fremont. We thank Maurits Burgering for help with the Mnt sample.

Aurantosides A and B: Cytotoxic Tetramic Acid Glycosides from the Marine Sponge *Theonella* sp.¹

Shigeki Matsunaga, Nobuhiro Fusetani,* and Yuko Kato

Laboratory of Marine Biochemistry
Faculty of Agriculture, University of Tokyo
Bunkyo-ku, Tokyo, Japan

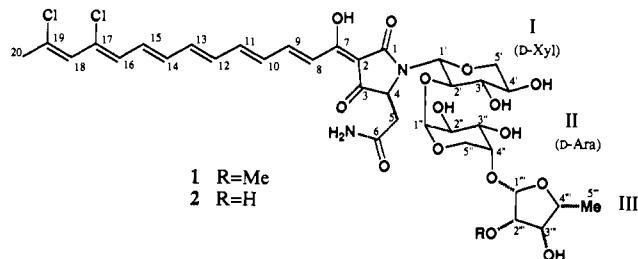
Hiroshi Hirota

Department of Chemistry, Faculty of Science
University of Tokyo, Bunkyo-ku, Tokyo, Japan
Received August 26, 1991

Certain sponges contain microbial symbionts including blue-green algae and bacteria² and possess secondary metabolites, some of which may be of microbial origin.³ A *Theonella* sponge collected off Hachijo Island, from which we isolated bioactive cyclic peptides,^{4,5} also contained orange pigments possessing cytotoxic activity. Here we describe the isolation and structure elucidation of the pigments named aurantosides A and B, which are superficially reminiscent of the streptolydigin.⁶

The MeOH extract of the sponge (15 kg) was partitioned between water and ether, and the aqueous phase was extracted with *n*-BuOH. The *n*-BuOH phase was gel-filtered over Sephadex LH-20 with MeOH. The cytotoxic orange band was purified by reverse-phase chromatography⁷ to furnish aurantioside A (**1**, 1.3 × 10⁻³% yield based on the wet weight) and aurantioside B (**2**, 1.5 × 10⁻³% yield),⁸ both as orange amorphous powders. They are cytotoxic against P388 and L1210 leukemia cells (1, IC₅₀ 1.8 and 3.4 μg/mL, respectively; 2, IC₅₀ 3.2 and 3.3 μg/mL).

The UV-visible spectrum of aurantioside A was pH-sensitive.⁸ **1** showed intense (M + Na)⁺ cluster ions with small (M + H)⁺



ion species in the FAB mass spectrum. A molecular formula of C₃₆H₄₆Cl₂N₂O₁₅ was established by the FAB mass and NMR spectral data, as well as from combustion analysis. A conjugated hexaene (C8-C20) was inferred from the COSY, HMQC, and HMBC spectra. Assignments for the olefinic protons and Me-20 were straightforward: signals were well separated, and long-range couplings were observed between H16 and H18 and between H18 and Me-20 in the normal COSY spectrum. Two chlorine atoms could be placed on C17 and C19 on the basis of their ¹³C chemical shifts (δ 129.8 and 137.4). Judging from the ¹H-¹H coupling constants and NOESY data, the double bonds have all-trans geometry.

Two apparent anomeric protons were shown in the ¹H and COSY spectra. Starting from the higher field signal (δ 5.04, d, J = 2.8 Hz), we could deduce an arabinopyranose structure (sugar II): H1'' and H4'' were equatorial, whereas H2'' and H3'' were axial. Another anomeric proton at δ 5.06 (H1''') was that of 5-deoxypentofuranose (sugar III), which had a methoxy group on C2''' as revealed by the HMBC spectrum. Interpretation of the NMR data for this unit was unexceptional. Though H1' and H2' signals of the sugar unit I were both broad and overlapping, ¹H-¹H coupling constants and NOESY data allowed us to assign the xylopyranose with an axial anomeric proton.⁹ This was supported by the COSY and NOESY spectra in CD₃OD at -30 °C, which gave well-separated and sharper signals for H1' and H2'.

The NMR spectra contained signals for a CHCH₂ unit (C4, C5) with a broadened methine proton. Two primary amide protons were observed in DMSO-*d*₆ which showed NOESY correlations with the C5 methylene protons, suggesting that a primary amide was attached to C5. The remaining portion (C1-C3 and C7) consisted of four nonprotonated carbons, generating broad signals at δ 195.0, 176.1, 174.8, and 102.0, one nitrogen and three oxygens. This constellation was reminiscent of a tetramic acid moiety, in which C4 is incorporated into the five-membered ring. The ¹³C chemical shifts agreed well with those reported for the relevant portion of streptolydigin.¹⁰ The above-mentioned structural units were connected, on the basis of HMBC spectral data (Table I). Structure **1** was fully consistent with the FAB-MS/MS data.¹¹

(9) Judging from the coupling constants, H2', H3', and H4' were all axial, so that this unit must be xylopyranose. In the NOESY spectrum, a strong correlation was observed between H5'a and a broad signal at δ 4.52 (H1' and H2'). H5'a and H2' project axially in opposite directions from the tetrahydropyran ring; therefore, this cross peak was assignable to the NOE between H5'a and H1'.

(10) Lee V. J.; Rinehart, K. L., Jr. *J. Antibiot.* **1980**, *33*, 408-415.

(11) The pseudomolecular ion peak at *m/z* 817 gave rise to ions at *m/z* 685, 555, and 423, which were generated by the cleavage of the three glycosidic bonds. Though the NMR data with broad ¹H and ¹³C signals indicate that aurantioside A exists as a mixture of four possible tautomers (2,3 enol or 2,7 enol with cis or trans 2,7 bond), X-ray study of a tetramic acid (Nolte, M. J.; Steyn, P. S.; Wessels, P. L. *J. Chem. Soc., Perkin Trans. 1* **1980**, 1057-1065) suggests that the tautomer depicted in formula **1** is the predominant one.

(1) Bioactive Marine Metabolites. 38. Part 37: Matsunaga, S.; Fusetani, N. *Tetrahedron Lett.* **1991**, *32*, 5605-5606.

(2) Trench, R. K. *Annu. Rev. Plant Physiol.* **1979**, *30*, 485-531.

(3) (a) Bergquist, P. R.; Wells, R. J. In *Marine Natural Products, Chemical and Biological Perspectives*; Scheuer, P. J., Ed.; Academic Press: New York, 1983; Vol. V., pp 1-50. (b) Hofheinz, W.; Oberhänsli, W. E. *Helv. Chim. Acta* **1977**, *60*, 660-669. (c) Frincke, J. M.; Faulkner, D. J. *J. Am. Chem. Soc.* **1982**, *104*, 265-269. (d) Matsunaga, S.; Fusetani, N.; Hashimoto, K.; Wälchli, M. *J. Am. Chem. Soc.* **1989**, *111*, 2582-2588.

(4) Fusetani, N.; Matsunaga, S.; Matsumoto, H.; Takebayashi, Y. *J. Am. Chem. Soc.* **1990**, *112*, 7053-7054.

(5) Fusetani, N.; Sugawara, T.; Matsunaga, S.; Hirota, H. *J. Am. Chem. Soc.* **1991**, *113*, 7811-7812.

(6) (a) Brill, G. M.; McAlpine, J. B.; Whittorn, D. *J. Antibiot.* **1988**, *41*, 36-44. (b) Meyers, E.; Cooper, R.; Dean, L.; Johnson, J. H.; Slusarchyk, D. S.; Trajo, W. H.; Singh, P. D. *J. Antibiot.* **1985**, *38*, 1642-1648 and references cited therein.

(7) The orange solids were first applied to an open column of ODS (70-230 mesh) and eluted with 30, 50, 70, 90, and 100% MeOH in water. The 90 and 100% MeOH fractions were combined and subjected to ODS HPLC with MeCN-H₂O (1:1) with 0.1% TFA to afford **1** and **2**.

(8) The name was coined from the Latin word aurantius, which means orange. **1**: amorphous solid, [α]_D²⁵ -568° (c = 0.1, MeOH); UV-vis (H₂O) 414 (ε 46 700), 242 nm (12 100); UV-vis (0.01 N HCl) 456 (ε 32 500), 324 nm (8500); UV-vis (0.01 N NaOH) 412 (ε 52 000), 241 nm (11 500); FAB-MS (positive) *m/z* 843, 841, 839 (M + Na)⁺, 821, 819, 817 (M + H)⁺; FAB-MS (negative) *m/z* 819, 817, 815 (M - H)⁻; IR (KBr) 3330, 2920, 1650, 1600, 1540, 1390, 1240, 1130, 1060, and 1000 cm⁻¹. **2**: amorphous solid, [α]_D²⁵ -492° (c = 0.1, MeOH); UV-vis (H₂O) 414 (ε 49 100), 242 nm (10 900); UV-vis (0.01 N HCl) 456 (ε 36 100), 301 nm (9800); UV-vis (0.01 N NaOH) 412 (ε 56 200), 242 nm (10 900); FAB-MS (positive) *m/z* 829, 827, 825 (M + Na)⁺, 807, 805, 803 (M + H)⁺; FAB-MS (negative) *m/z* 805, 803, 801 (M - H)⁻; IR (KBr) 3320, 2900, 1650, 1610, 1540, 1390, 1230, 1130, 1070, 1040, and 995 cm⁻¹.